AD-OX: A sequential oxidative process for water treatment- adsorption and batch CWAO regeneration of activated carbon

H. Delmas*, C. Creanga, C. Julcour-Lebigue, and A.-M. Wilhelm
Laboratoire de Génie Chimique, Université de Toulouse, INPT
5 rue Paulin Talabot, 31106 Toulouse, France
*Corresponding author: henri.delmas@ensiacet.fr, tel.: +33 5 62 88 58 88; fax: +33 5 34 61 52 53.

Abstract

A sequential process for water treatment involving usual adsorption on activated carbon (AC) followed by wet air catalytic oxidation of the adsorbed pollutants has been carried out in a fixed bed reactor with a mixture of two model pollutants. The first step achieves water purification while the second one reduces the organic pollution but also, more importantly, performs some AC in situ regeneration.

The experimental work has been done with AC yet extensively used and stabilized by long range continuous oxidation. The two steps have been analysed successively showing very important drop of adsorption capacity with respect to fresh AC but efficient oxidative partial regeneration. As expected with used AC no more evolution occurs in between two consecutive runs. The first step of competitive adsorption has been simulated by a model leading to higher diffusivities than estimations based on correlations. The main features of the complex second step, involving simultaneous non isothermal desorption and three phase catalytic reaction, are qualitatively explained.

Keywords: Adsorption; Catalytic oxidation; Activated carbon; Water treatment; Multiphase reactions; Packed bed; Mathematical modelling

1. Introduction

Wastewater treatment is a growing issue for sustainable development. Specially, cheap and reliable processes should be developed to match the future specifications on both the toxic organic compounds and the global Chemical Oxygen Demand (COD).

The most usual processes to carry out industrial water treatment are biodegradation and/or physicochemical treatment. To achieve further separation of the less biodegradable organic compounds, adsorption on activated carbon is usually carried out as a final treatment. Nevertheless this powerful technique, with regards to organic pollutant separation, highly suffers from economy and sustainability aspects, as the saturated activated carbon is either hardly regenerated - by non environmental friendly ex situ high temperature processes - or even, most often for industrial wastewater, it becomes itself a solid waste to be incinerated.

Therefore new methods have been investigated by researchers for the treatment and recovery of spent activated carbons (ACs). They are mostly based on chemical regeneration, performed either by desorption of fixed pollutants using specific solvents or by decomposition of the adsorbates with oxidizing/reducing agents.

Extraction with solvents requires further separation such as distillation to remove the extracted contaminants and recycle the solvents. Advanced oxidation processes (AOPs) using hydrogen peroxide or Fenton's reagent are quite promising technologies for the recovery of

used carbon owing to their potency to degrade a wide range of organic pollutants by the generation of very reactive and non selective free hydroxyl radicals [1-3]. However they require extra reagents which greatly increase their operating cost. Ozone utilization leads to interactions between ozone and AC which may affect its structural and chemical properties resulting in a decrease of its adsorption capacity [4]. Impregnation of the ACs with metal oxides has also been proposed to promote decomposition of adsorbed contaminants by catalytic air oxidation [5-6].
Recently commercial AC has been successfully applied as a direct catalyst in Catalytic Wet Air Oxidation (CWAO) for the destruction of phenolic compounds [7-11]. AC can even perform better than supported catalysts based on the transition metals [7], probably due to its high adsorption capacity combined to oxygen-containing surface groups.
In this work a sequential process [12,13] for (post)treatment of water polluted by non biodegradable organic compounds has been investigated. It is based on hybridizing classical adsorption on a fixed bed of activated carbon followed by batch wet catalytic oxidation at higher temperature and pressure on the same bed of AC, which is then regenerated in situ.
The basic idea is to take advantage of both operations: 1-efficient and cheap water purification at room temperature by adsorption, 2-effective pollutant degradation by batch air oxidation achieving simultaneously some AC regeneration for the next adsorption. Compared to usual continuous oxidation [14] only a small fraction of the wastewater to be treated has to be heated in this batch CWAO and very high conversion is no longer required as water quality is provided by the adsorption step. These advantages are more valuable at low pollutant concentration, i.e. after conventional biological treatment. When comparing now with usual adsorption with spent AC significant AC savings are expected. This new process should be especially beneficial in the highest concentration range of usual adsorption and/or in the lower concentration range of continuous CWAO process.

In most academic works dealing with oxidative water treatments, model pollutants have been used for analytical and scientific reasons in order to better quantify the process efficiency and its possible by-products. Among the model pollutants phenol is undoubtedly the most popular one [15,16]; nevertheless a few papers have investigated the catalytic oxidation of substituted phenols: 2- and 4-chlorophenol and 4-nitrophenol on supported metal oxides [17,18], 2-aminophenol, salicylic acid, 5-sulfo salicylic acid, nitrophenols, cresols and chlorophenols on AC [10,19,20], 2-chlorophenol, 4-coumaric, 4-hydroxyphenylacetic and 4-hydroxybenzoic acids over Pt and Ru supported catalysts [21-24].
4-hydroxybenzoic acid (4HBA) is of special interest as typically found in oxidative treatments of wastes of olive oil industry [25]. It is considered especially toxic and refractory to usual wastewater biological treatment [26]. It is also an unexpected intermediate product of phenol oxidation on AC [8,9].
Most often wastewaters are mixtures of several pollutants. To investigate the feasibility of the AD-OX process with complex mixtures, a model mixture of phenol and 4HBA has been treated in this work, following previous studies on batch and continuous CWAO of phenol [9] and 4-hydroxybenzoic acid [27,28] on activated carbon.

2. Experimental

The experimental set-up (Figure 1) has been derived from a continuous CWAO equipment, yet detailed in Suwanprasop *et al.* [9]. The main change concerns the liquid flow which may successively enter and leave the reactor, during the adsorption step, or be recycled through a batch loop including a pressurized tank (3), during the heating, reaction and cooling steps.

The fixed bed reactor (1) consists of a jacketed column of 1.2 m high and 0.025 m internal diameter. It is packed with 0.325 kg of activated carbon particles (Merck 2514, [1.25-1.60]$\cdot 10^{-3}$ m sieved fraction).
Note that the experiments have not been carried with fresh activated carbon. In order to avoid an unknown period of AC stabilization, this work was indeed achieved with aged AC, yet extensively used in the same fixed bed (similar temperature and pressure conditions, same model pollutants) for many continuous oxidation runs, thus undergoing continuous simultaneous adsorption – oxidation for more than 300hrs. It has been verified that this used AC has reached a quasi steady state by repeating experiments in reference conditions [28].
It has also been estimated that AC consumption by direct oxidation is very limited as discussed below. The weight of the aged AC used in this work was 20% higher than the fresh AC introduced in the reactor before preliminary continuous oxidation runs. On another hand the weight loss during TGA experiments was approximately 17% between 100°C and 700°C on aged AC (20% heavier) and 1.5% on fresh AC. So the TGA weight loss difference (about 19%) is approximately equal to the weight increase from fresh to aged AC, suggesting that very few carbon has been consumed during all the oxidation runs (continuous and batch at the end).

Nine temperature probes (T) and eight sample valves (10) are located at different reactor heights to get axial profiles of temperature and liquid concentrations respectively. Additionally, liquid sampling is done after the gas-liquid separator.
The reactor can operate with either down flow or up flow of gas-liquid according to the position of five three way valves (V1 to V5) located along the gas and liquid circuits. A flexible grid is put at the top of the reactor to prevent fluidization of particles during the up flow operation. Here only up flow has been used.
During the adsorption step the solution of equimolar mixture of phenol and 4-hydroxybenzoic acid (25.8 mol.m^{-3} each) is fed to the column at atmospheric pressure by a dosing pump (8) from a weighted tank (6).
During the batch reaction step the same pump is used to recycle the reaction mixture at higher temperature and pressure through the pressurized tank (3) and gas supply is achieved by two mass flow-controllers allowing different gas mixtures. The wall temperature is set at 413 K and the total operating pressure at 6 bar. Gas flow rate is $2.78\cdot 10^{-5}$ m^3.s^{-1} (NTP), corresponding to an inlet gas velocity of about 10^{-2} m.s^{-1}. By using a 85/15 composition of the O_2/N_2 inlet mixture, oxygen partial pressure is adjusted at 2 bar (equilibrium pressure at reactor outlet). Liquid space time varies from 0.1 to 0.7 h (liquid velocities of $0.25\cdot 10^{-3}$ to $1.2\cdot 10^{-3}$ m.s^{-1}). These conditions correspond to the bubble flow regime or transition to pulsed flow regime in the selected up flow mode.
During the two steps, liquid samples are regularly withdrawn at the bed outlet. They are analyzed by HPLC using a C18 reverse phase column (ProntoSIL C18 AQ) and a dual wavelength UV detector (UV2000 Thermo Finnigan) to obtain concentrations of phenol and 4HBA. The separation of those compounds from the oxidation intermediates is achieved with a mobile phase of variable composition programmed at 1 mL/min, using acidified deionised water and acetonitrile as eluants.
Three successive cycles - adsorption steps at room temperature, followed by heating and pressurization, then batch oxidation with liquid recycle, and final cooling prior to next adsorption - have been performed for the phenol-4HBA mixture at different liquid flow rates.

3. Results and discussion

3.1. Adsorption.

In this work, as shown on breakthrough curves (Figure 2), the adsorption step has been achieved up to complete AC saturation, contrary to a true AD-OX operation where the polluted water fed should be stopped when the pollutant concentration reaches the accepted threshold. Indeed the complete saturation provides a better knowledge of the adsorption performance of this used activated carbon and allows the comparison with simulations of the adsorption step, while in the actual AD-OX process this step should stop as soon as the pollutant concentration reaches the accepted limit.

First it should be noticed that the two consecutive experiments give very reproducible breakthrough curves, which confirms the stabilization of the activated carbon both as adsorbent and as oxidation catalyst. It should be remembered that this stable behavior may only be observed on used catalyst while fresh activated carbon undergoes a severe drop of adsorption capacity after the first oxidation [27].

Concerning adsorption selectivity, phenol adsorbs faster but is progressively removed by 4HBA in agreement with competitive adsorption data showing preferential 4HBA adsorption [29]. This selectivity can be explained by the much lower solubility of 4HBA in water (about 20 times less than phenol).

The dynamics of this competitive adsorption has been simulated by a model including adsorption equilibria (isotherms), pore diffusion, liquid–solid mass transfer and liquid axial dispersion through series of CSTR with the following assumptions:

- Surface diffusion in pores is not taken into account (only usual pore diffusion).
- External liquid–solid mass transfer coefficient is calculated by Ranz and Levenspiel correlation [30].
- The number of CSTR in series is calculated with the Bodenstein Number (or particle Peclet Number) of 0.5 as usually accepted. Here, it gives 241 tanks in series.
- Adsorption is very fast: at any depth in pores local adsorption equilibrium is assumed. This equilibrium is represented by the two simplified Langmuir adsorption isotherms (eq. 1 and 2 where A stands for 4HBA and B for phenol):

$$q_A = \frac{q_{\max} \cdot K_{L,A} \cdot C_A}{1 + K_{L,A} \cdot C_A + K_{L,B} \cdot C_B} \tag{1}$$

$$q_B = \frac{q_{\max} \cdot K_{L,B} \cdot C_B}{1 + K_{L,A} \cdot C_A + K_{L,B} \cdot C_B} \tag{2}$$

which have been proved convenient for this competitive adsorption on the fresh Merck activated carbon.

In this model the initial conditions assume no remaining phenol and 4HBA on the activated carbon though the previous batch oxidation cannot be completely achieved (it is stopped when the concentration of pollutant in the liquid phase reaches 10% or less of initial feed concentration, cf. Figure 5).

The local mass balances inside a spherical AC particle of the i^{th} tank gives

$$\varepsilon'_p \cdot \frac{\partial C_{A,i}}{\partial t} + \rho'_p \cdot \frac{\partial q_{A,i}}{\partial t} = \frac{D'_{e,A}}{r^2} \cdot \frac{\partial}{\partial r}\left(r^2 \cdot \frac{\partial C_{A,i}}{\partial r} \right) \tag{3}$$

$$\varepsilon'_p \cdot \frac{\partial C_{B,i}}{\partial t} + \rho'_p \cdot \frac{\partial q_{B,i}}{\partial t} = \frac{D'_{e,B}}{r^2} \cdot \frac{\partial}{\partial r}\left(r^2 \cdot \frac{\partial C_{B,i}}{\partial r} \right) \quad (4)$$

ε'_p et ρ'_p are the porosity and apparent density of aged AC (ε'_p = 0.31; ρ'_p = 1251 kg.m^{-3}) which are found significantly different from that of fresh AC (ε_p = 0.59; ρ_p = 1032 kg.m^{-3}). Those properties have been calculated from pore volume and structural density measured with nitrogen sorption analyzer and helium pycnometer respectively.

The effective pore diffusivity of compound j ($D'_{e,j}$) is obtained from its molecular diffusivity in water ($D_{m,j}$) according to:

$$D'_{e,j} = \frac{\varepsilon'_p}{\tau_p} D_{m,j} \quad (5)$$

with τ_p the pore tortuosity of the catalyst particles.

Boundary conditions

- $\forall\, t,\ r = 0,\ \dfrac{\partial C_{A,i}}{\partial r} = 0$ (spherical symmetry) (6)

$$\frac{\partial C_{B,i}}{\partial r} = 0 \quad (7)$$

- $t,\ r = d_p/2,\ k_{LS,A} \cdot \left(C_{LA,i} - C_{SA,i}\right) = D'_{e,A} \cdot \left(\dfrac{\partial C_{A,i}}{\partial r} \right)_{r=d_p/2}$ (8)

$$k_{LS,B} \cdot \left(C_{LB,i} - C_{SB,i}\right) = D'_{e,B} \cdot \left(\frac{\partial C_{B,i}}{\partial r} \right)_{r=d_p/2} \quad (9)$$

The mass balance on the liquid phase (out of particles) of the ith tank gives:

$$\frac{\varepsilon_B \cdot V_R}{N_{cell}} \cdot \frac{dC_{LA,i}}{dt} = k_{LS,A} \cdot \frac{6}{d_p} \cdot (1-\varepsilon_B) \cdot \left(C_{SA,i} - C_{LA,i}\right) \cdot \frac{V_R}{N_{cell}} - Q_L \cdot \left(C_{LA,i} - C_{LA,i-1}\right) \quad (10)$$

$$\frac{\varepsilon_B \cdot V_R}{N_{cell}} \cdot \frac{dC_{LB,i}}{dt} = k_{LS,B} \cdot \frac{6}{d_p} \cdot (1-\varepsilon_B) \cdot \left(C_{SB,i} - C_{LB,i}\right) \cdot \frac{V_R}{N_{cell}} - Q_L \cdot \left(C_{LB,i} - C_{LB,i-1}\right) \quad (11)$$

A four point orthogonal collocation method has been used to approximate spatial derivatives (inside the pellet) and the resulting system of equations has been solved using the Gear method. A Gauss Newton technique for optimizing the unknown (isotherm) parameters by matching the exit concentration profiles of the two adsorbed species is then carried out.

Concerning the result analysis the main point is that the model cannot fit the experimental breakthrough curves when using effective pore diffusivities based on Wilke-Chang correlation for molecular diffusivity of 4HBA and phenol in water, and usual values of tortuosity factor (τ_p = 2-3). It should be noticed that the same problem occurred when trying to simulate the dynamics of batch adsorption experiments of fresh AC in stirred vessel [29]. In both cases effective diffusivities should be significantly increased. Here diffusivities are thus also optimized, keeping the 4HBA/phenol diffusivity ratio as obtained from Wilke-Chang correlation. All optimized data are presented in Table 1.

Optimization tests have proved the three adsorption parameters to be less sensitive than diffusivity, here varied through the pore tortuosity factor τ_p while keeping Wilke-Chang correlation. Figure 3 shows the best fit of the model with the breakthrough curves, with faster initial adsorption of phenol due to higher diffusivity, followed by its removal due to higher 4HBA affinity to AC. The best fit being obtained with τ_p = 0.64 means that optimized diffusivities are at least three times higher than expected ones. This significant disagreement may be attributed not only to this questionable correlation but even more to the particle size distribution and measurement and to the spherical particle hypothesis, as well as to the possible effect of surface diffusion.

An important and negative result should be pointed out: this used AC has lost a large part of its potential adsorption capacity as it has been divided by about 6 compared to the same fresh AC. Indeed according to co-adsorption results using different initial proportions of the two pollutants and modelling of the corresponding data by a generalized Langmuir isotherm, the theoretical adsorption capacity of fresh AC in equilibrium with feed concentrations should be $q_{e,phenol}$ = 0.17 mol.kg^{-1} $_{AC}$ and $q_{e,4HBA}$ = 2.09 mol.kg^{-1} $_{AC}$ [29].
The lower adsorption capacity of aged AC (cf. Table 1) is due to accumulation of heavy polyphenols irreversibly adsorbed on AC and hardly oxidized later, resulting in a significant loss of BET surface area, from 980 m^2/g to 250 m^2/g. Similar drop of adsorption capacity has been already observed on various ACs using various aromatic pollutants even after much less oxidation time. Successive adsorption and oxidation runs in autoclave reactor, starting with fresh AC, suggest that the main adsorption drop occurs after the first oxidation followed by quasi steady behaviour both for oxidation and adsorption.

Finally the optimized values not only match reasonably well with the breakthrough curves but also with adsorption equilibrium data of 4HBA measured on this aged AC after it has been washed with bidistilled water during several days - so that to eliminate all reversibly-adsorbed components - and dried (Figure 4).

3.2. Oxidation

Starting from complete AC saturation, batch oxidations were performed, at p_{O2} = 2 bar and T = 413 K, and at two different liquid flow rates ($5.56 \cdot 10^{-7}$ and $1.39 \cdot 10^{-7}$ m^3.s^{-1}). Batch oxidation curves are shown in Figure 5. Due to significant initial desorption at higher temperature (413 K instead of 298 K, approximately as on Fig. 4, where this temperature effect is shown for fresh AC) the concentration profiles start at higher concentrations than 25.8 mol.m^{-3}, the equimolar concentration of pollutants. This batch CWAO being carried out during three days with stops by night, some peaks are found when starting heating again (e.g at 550 min) due to subsequent desorption.
A clear understanding of the two concentration variations with time, based on a complete modeling of all phenomena is not yet possible contrary to continuous CWAO.

First, it should be recalled that liquid concentrations vary due to two main reasons: oxidation and desorption. Due to the relative high solid loading of this kind of batch recycle reactor, the two compounds are mostly adsorbed on AC and only a small fraction appears in the aqueous phase. Adsorption isotherms for the mixture on this particular used AC at high temperature are not available. Nevertheless they have been performed in stirred autoclave on the same Merck AC but being stabilized after several oxidation runs in the autoclave using thus a different liquid/solid ratio than in the fixed bed [28].

Second, intrinsic kinetics have been obtained again with slightly differently aged ACs for both 4HBA and 4HBA-phenol mixture [28]. This paper enlightens a commonly ignored effect of adsorption on catalytic reaction kinetics determination from batch measurements: the mass balance should take into account the variation of the adsorbed reactant content on the catalyst and not only the concentration variations in the liquid phase. It was shown that intrinsic kinetics derived when ignoring this variable adsorbed content may lead to large errors concerning the rate constants. Here due to the very high solid loading this adsorption effect is predominant. So, in this AD-OX oxidation step, the much faster phenol concentration decrease during oxidation is due to lower adsorbed amount and not to intrinsic kinetics, which proved phenol and 4HBA to be very similarly oxidized [28].

Faster oxidation at low liquid flow rate may appear surprising. Here again a complete explanation through a model would be useful. Nevertheless it should be pointed out that low liquid recycle flow corresponds to higher temperature profile in the fixed bed reactor, as presented on Figure 6, showing axial temperature profiles when steady state has been reached, while Figure 7 shows the temperature transients after starting heating. This steeper temperature profile at low liquid flow rate is likely the most relevant explanation of the better performance of the oxidation step in this condition: a larger part of the bed is catalytically active.

4. Conclusions

A sequential oxidation-adsorption process using a commercial activated carbon without pre-treatment and operating in mild conditions has been applied for the remediation of a pollutant mixture. Due to complex simultaneous non isothermal oxidation and desorption phenomena on aged AC the oxidative regeneration step cannot be simulated, contrary to continuous oxidation [9,29] and to isothermal adsorption. Nevertheless the main features may be qualitatively understood.

Compared to fresh AC the adsorption capacity with this used AC has been dramatically decreased to about 15%. Nevertheless this limited adsorption capacity may be fully recovered by batch CWAO, AC playing then the role of catalyst of its own regeneration.

In the mini pilot plant previously built for continuous CWAO the adsorption time is extremely low (1/2 h) compared to the regeneration time (25 h). A convenient plant to investigate this process on actual industrial wastewater should then have a much higher AC loading to increase the adsorption time while the batch reaction time is constant. For example to have similar adsorption and heating-oxidation-cooling times the AC weight should be fifty to hundredfold. A two parallel column plant with alternative adsorption - regeneration steps should then be operated to carry out continuous water treatment.

Notation

C_j	concentration of compound j ($mol.m^{-3}$)
C_{Lj}	concentration of compound j in the bulk liquid phase ($mol.m^{-3}$)
C_{Sj}	liquid-phase concentration of compound j on the catalyst surface ($mol.m^{-3}$)
$D'_{e,j}$	effective diffusion coefficient of compound j in aged AC pores ($m^2.s^{-1}$)
$D_{m,j}$	molecular diffusivity of compound j in water ($m^2.s^{-1}$)

d_p	catalyst particle diameter (m)
$K_{L,j}$	isotherm constant of compound j ($m^3.mol^{-1}$)
$k_{LS,j}$	j-compound liquid – solid mass transfer coefficient ($m.s^{-1}$)
N_{cell}	number of CSTR in series
p_{O2}	oxygen partial pressure (bar)
$q_{e,j}$	adsorbed amount of compound j on AC in equilibrium with feed concentration ($mol.kg^{-1}_{AC}$)
q_j	adsorbed amount of compound j on AC ($mol.kg^{-1}_{AC}$)
Q_L	liquid flow rate ($m^3.s^{-1}$)
q_{max}	maximum adsorption capacity of AC ($mol.kg^{-1}_{AC}$)
r	particle radial coordinate (m)
t	time (s)
T	temperature (K)
V_R	reactor volume (m^3)
Greek	
ε_B	catalyst bed void fraction
ε_p	catalyst porosity
ε'_p	aged catalyst porosity
ρ_p	catalyst particle density ($kg.m^{-3}$)
ρ'_p	aged catalyst particle density ($kg.m^{-3}$)
τ_p	pore tortuosity
Subscripts	
AC	activated carbon
4HBA	4-hydroxybenzoic acid
i	i^{th} tank
L	liquid
p	particle
PZC	point of zero charge

Acknowledgements

EC through the 6th FP "REMOVALS" and ANR-Precodd "PHARE" are acknowledged.

References

[1] L.C. Toledo, A.C. Bernardes Silva, R. Augusti, R. Montero Lago, Application of Fenton's reagent to regenerate activated carbon saturated with organochloro compounds, Chemosphere 50 (2003) 1049–1054.

[2] S.G. Huling, P.K. Jones, W.P. Ela, R.G. Arnold, Fenton-driven chemical regeneration of MTBE-spent GAC, Water Res. 39 (2005) 2145–2153.

[3] K. Okawa, K. Suzuki, T. Takeshita, K. Nakano, Regeneration of granular activated carbon with adsorbed trichloroethylene using wet peroxide oxidation, Water Res. 41 (2007) 1045–1051.

[4] P.M. Alvarez, F.J. Beltran, V. Gomez-Serrano, J. Jaramillo, E.M. Rodriguez, Comparison between thermal and ozone regenerations of spent activated carbon exhausted with phenol, Water Res. 38 (2004) 2155–2165.

[5] Y.I. Matatov-Meytal, M. Sheintuch, Abatement of Pollutants by Adsorption and Oxidative Catalytic Regeneration, Ind. Eng. Chem. Res. 36 (10) (1997) 4374-4380.

[6] M. Sheintuch, Y.I. Matatov-Meytal, Comparison of catalytic processes with other regeneration methods of activated carbon, Catal. Today 53 (1999) 73–80.
[7] A. Fortuny, J. Font, A. Fabregat, Wet air oxidation of phenol using active carbon as catalyst, Appl. Catal. B: Environ. 19 (3-4) (1998) 165-173.
[8] A. Eftaxias, J. Font, A. Fortuny, A. Fabregat, F. Stüber, Catalytic wet air oxidation of phenol over active carbon catalyst. Global kinetic modelling using simulated annealing, Appl. Catal. B: Environ. 67 (1-2) (2006) 12-23.
[9] S. Suwanprasop, A. Eftaxias, F. Stüber, I. Polaert, C. Julcour-Lebigue, H. Delmas, Scale-up and modeling of fixed bed reactors for the catalytic phenol oxidation over adsorptive active carbon, Ind. Eng. Chem. Res. 44 (2005) 9513-9523.
[10] M.E. Suarez-Ojeda, F. Stüber, A. Fortuny, A. Fabregat, J. Carrera, J. Font, Catalytic wet air oxidation of substituted phenols using active carbon catalyst, Appl. Catal. B: Environ. 58 (1-2) (2005) 105-114.
[11] A. Santos, P. Yustos, T. Cordero, S. Gomis, S. Rodriguez, F. Garcia-Ochoa, Catalytic wet air oxidation of phenol on active carbon: stability, phenol conversion and mineralization, Catal. Today 102-103 (2005) 213-218.
[12] H. Delmas, A.M. Wilhelm, I. Polaert, A. Fabregat, F. Stüber, J. Font, Sequential process of adsorption and catalytic oxidation on activated carbon for (pre)treatment of water polluted by non-biodegradable organic products, French patent FRXXBL FR 2826356 A1 20021227, 2002.
[13] I. Polaert, A.M. Wilhelm, H. Delmas, Phenol wastewater treatment by a two-step adsorption-oxidation process on activated carbon, Chem. Eng. Sci. 57 (9) (2002) 1585-1590.
[14] F. Stüber, J. Font, A. Fortuny, C. Bengoa, A. Eftaxias, A. Fabregat, Carbon materials and catalytic wet air oxidation of organic pollutants in wastewater, Top. Catal. 33 (1-4) (2005) 3-50.
[15] A. Pintar, J. Levec, Catalytic liquid-phase oxidation of phenol aqueous solutions. A kinetic investigation, Ind. Eng. Chem. Res. 33 (12) (1994a) 3070-3077.
[16] F. Stüber, I. Polaert, H. Delmas, J. Font, A. Fortuny, A. Fabregat, Catalytic wet air oxidation of phenol using active carbon: performance of discontinuous and continuous reactors, J. Chem. Technol. Biotechnol. 76 (2001) 743-751.
[17] A. Pintar, J. Levec, Catalytic oxidation of aqueous p-chlorophenol and p-nitrophenol solutions, Chem. Eng. Sci. 49 (24) (1994b) 4391-4407.
[18] D. Posada, P. Betancourt, F. Liendo, J.L. Brito, Catalytic wet air oxidation of aqueous solutions of substituted phenols, Catal. Lett. 106 (1-2) (2006) 81-88.
[19] V. Tukac, J. Hanika, Catalytic wet oxidation of substituted phenols in the trickle bed reactor, J. Chem. Technol. Biotechnol. 71 (1998) 262-266.
[20] A. Santos, P. Yustos, S. Rodriguez, F. Garcia-Ochoa, Wet oxidation of phenol, cresols and nitrophenols catalyzed by activated carbon in acid and basic media, Appl. Catal. B: Environ. 65 (3-4) (2006) 269-281.
[21] Y. Kojima, T. Fukuta, T. Yamada, M.S. Onyango, E.C. Bernardo, H. Matsuda, K. Yagishita, Catalytic wet oxidation of o-chlorophenol at mild temperatures under alkaline conditions, Water Res. 39 (1) (2005) 29-36.
[22] N. Li, C. Descorme, M. Besson, Catalytic wet air oxidation of aqueous solution of 2-chlorophenol over Ru/zirconia catalysts, Appl. Catal. B: Environ. 71 (3-4) (2007) 262-270.
[23] D. Pham Minh, P. Gallezot, M. Besson, Degradation of olive oil mill effluents by catalytic wet air oxidation: 1- Reactivity of p-coumaric acid over Pt and Ru supported catalysts, Appl. Catal. B: Environ. 63 (1-2) (2006) 68-75.
[24] D. Pham Minh, G. Aubert, P. Gallezot, M. Besson, Degradation of olive oil mill effluents by catalytic wet air oxidation: 2- Oxidation of p-hydroxyphenylacetic and p-hydroxybenzoic acids over Pt and Ru supported catalysts, Appl. Catal. B: Environ. 73 (3-4) (2007) 236-246.

[25] J. Beltran-Heredia, J. Torregrosa, J.R. Dominguez, J.A. Peres, Comparison of the degradation of p-hydroxybenzoic acid in aqueous solution by several oxidation processes, Chemosphere 42 (4) (2001) 351-359.
[26] M.D. Gonzalez, E. Moreno, J. Quevedo-Sarmiento, A. Ramos-Cormenzana, Studies on antibacterial activity of waste waters from olive oil mills (alpechin): inhibitory activity of phenolic and fatty acids, Chemosphere 20 (3-4) (1990) 423-432.
[27] C. Creanga Manole, C. Julcour-Lebigue, A.M. Wilhelm, H. Delmas, Catalytic oxidation of 4-hydroxybenzoic acid on activated carbon in batch autoclave and fixed bed reactor, Ind. Eng. Chem. Res. 46 (25) (2007a) 8388-8396.
[28] C. Creanga Manole, C. Ayral, C. Julcour-Lebigue, A.M. Wilhelm, H. Delmas, Catalytic wet air oxidation of aqueous organic mixtures, Int. J. Chem. React. Eng. 5 (2007b) A65, http://www.bepress.com/ijcre/vol5/A65
[29] C. Creanga Manole, AD-OX Process for remediation of non biodegradable organic pollutants (by adsorption then catalytic oxydation), Ph-D thesis, INP Toulouse, France, 2007, http://ethesis.inp-toulouse.fr/archive/00000561/
[30] D. Kunii, O. Levenspiel, Fluidization Engineering, Wiley, 1969.

TABLE CAPTIONS

Table 1. Optimized parameters of generalized Langmuir adsorption of 4HBA – phenol and corresponding adsorption capacities at equilibrium with the equimolar solution.

FIGURE CAPTIONS

Figure 1. AD-OX experimental set up.

1 jacketed packed bed column, **2** gas-liquid separator, **3** pressurized liquid storage tank, **4** condenser, **5** gas mass-flow controllers, **6** feed tank, **7** balance, **8** dosing pump, **9** sampling device, **10** liquid sample valves, **11** pneumatic valve, **12** expansion vase, **13** gear pump, **14** heater, **15** cooling exchanger, **16*** cooling exchanger, **17*** anti-pulsatory vessel, **18*** flowmeter, **V1-V5** three-way valves for up- or down-flow mode.

Figure 2. Successive breakthrough curves with equimolar phenol-4HBA mixture (Q_L=8.33·10^{-7} m^3.s^{-1}, T=298K). 1st breakthrough: 4HBA (◇) and phenol (□) outlet concentrations; 2nd breakthrough: 4HBA (◆) and phenol (■) outlet concentrations.

Figure 3. Comparison of experimental and simulated breakthrough curves. Dots: experimental 4HBA (◇) and phenol (□) outlet concentrations; lines: simulated breakthrough curves for 4HBA (dashed) and phenol (continuous).

Figure 4. Adsorption isotherms of 4HBA on fresh AC at 298 K (◆) and 423 K (◇) and on aged AC at 298 K (○) [continuous lines: Langmuir models for fresh AC, dashed line: fitted generalized Langmuir model ($C_{e,phenol}$ = 0) for aged AC].

Figure 5. Evolution of 4HBA (◇) and phenol (□) concentration during batch CWAO at two liquid recycle flow rates: Q_L = 5.56·10^{-7} m^3.s^{-1} (gray filled symbols) and Q_L = 1.39·10^{-7} m^3.s^{-1} (black filled symbols) [t=0 corresponds to the introduction of O_2/N_2 mixture].

Figure 6. Steady state axial temperature profiles at two liquid recycle flow rates: Q_L = 5.56·10^{-7} m^3.s^{-1} (□) and Q_L = 1.39·10^{-7} m^3.s^{-1} (◆).

Figure 7. Time evolution of temperature at different axial positions after starting heating: Z=0 (■), Z=0.12 m (▲), Z=0.36 m (◆), Z=0.6 m (●), Z=0.84 m (□), Z=1.08 m (△), Z=1.2 m (○) [Q_L = 1.39·10^{-7} m^3.s^{-1}].

Table 1

q_{max} (mol.kg$^{-1}_{AC}$)	$K_{L,phenol}$ (m^3.mol^{-1})	$K_{L,4HBA}$ (m^3.mol^{-1})	τ_p	$q_{e,phenol}$ (mol.kg$^{-1}_{AC}$)	$q_{e,4HBA}$ (mol.kg$^{-1}_{AC}$)
0.65	0.013	0.039	0.64	0.092	0.28

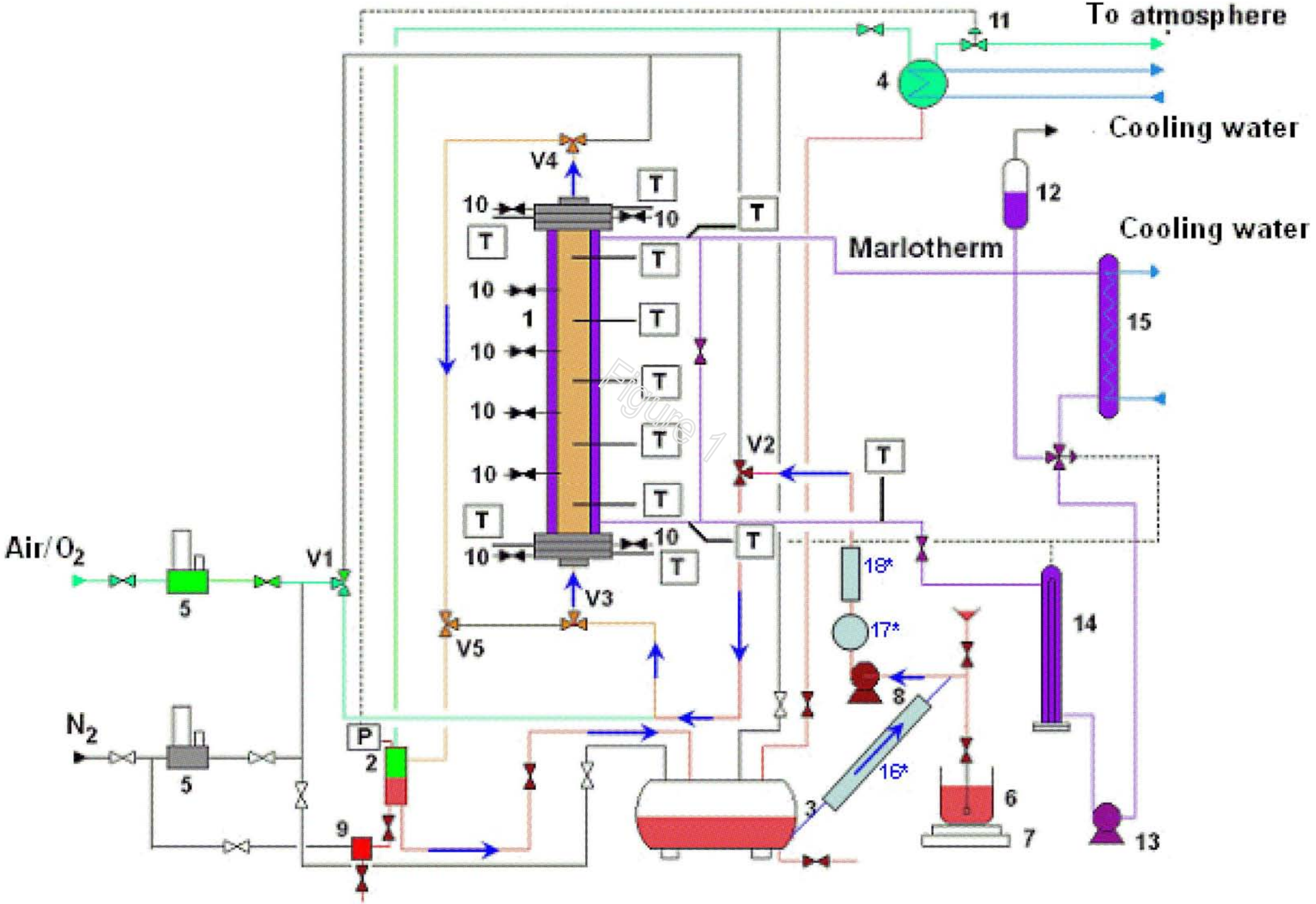
To atmosphere
Cooling water
Cooling water
Marlotherm
Air/O_2
N_2
V1
V2
V3
V4
V5
1
2
3
4
5
6
7
8
9
10
11
12
13
14
15
16*
17*
18*
P
T

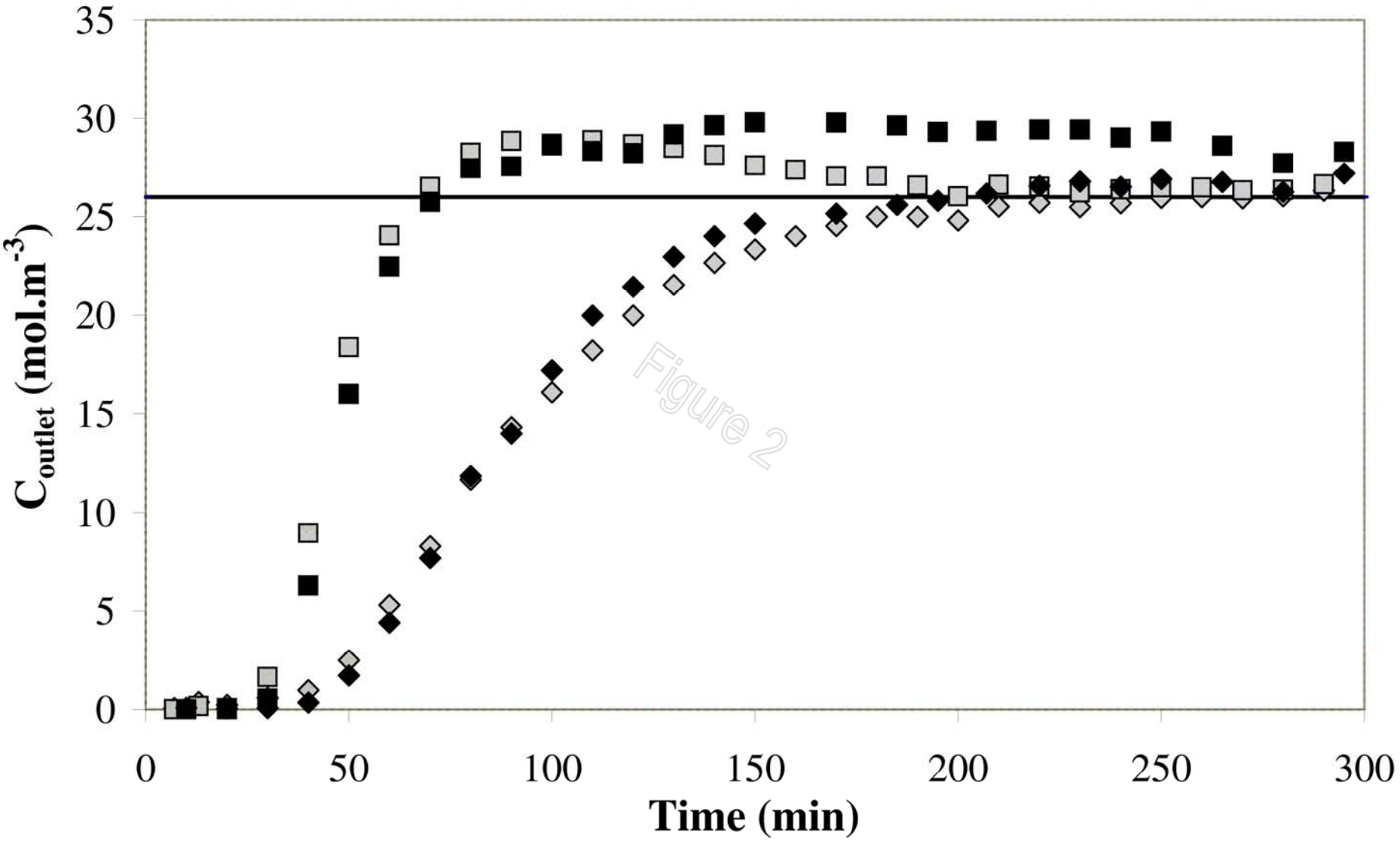
35
30
25
20
15
10
5
0
0
50
100
150
200
250
300
C_{outlet} (mol.m^{-3})
Time (min)
Figure 2

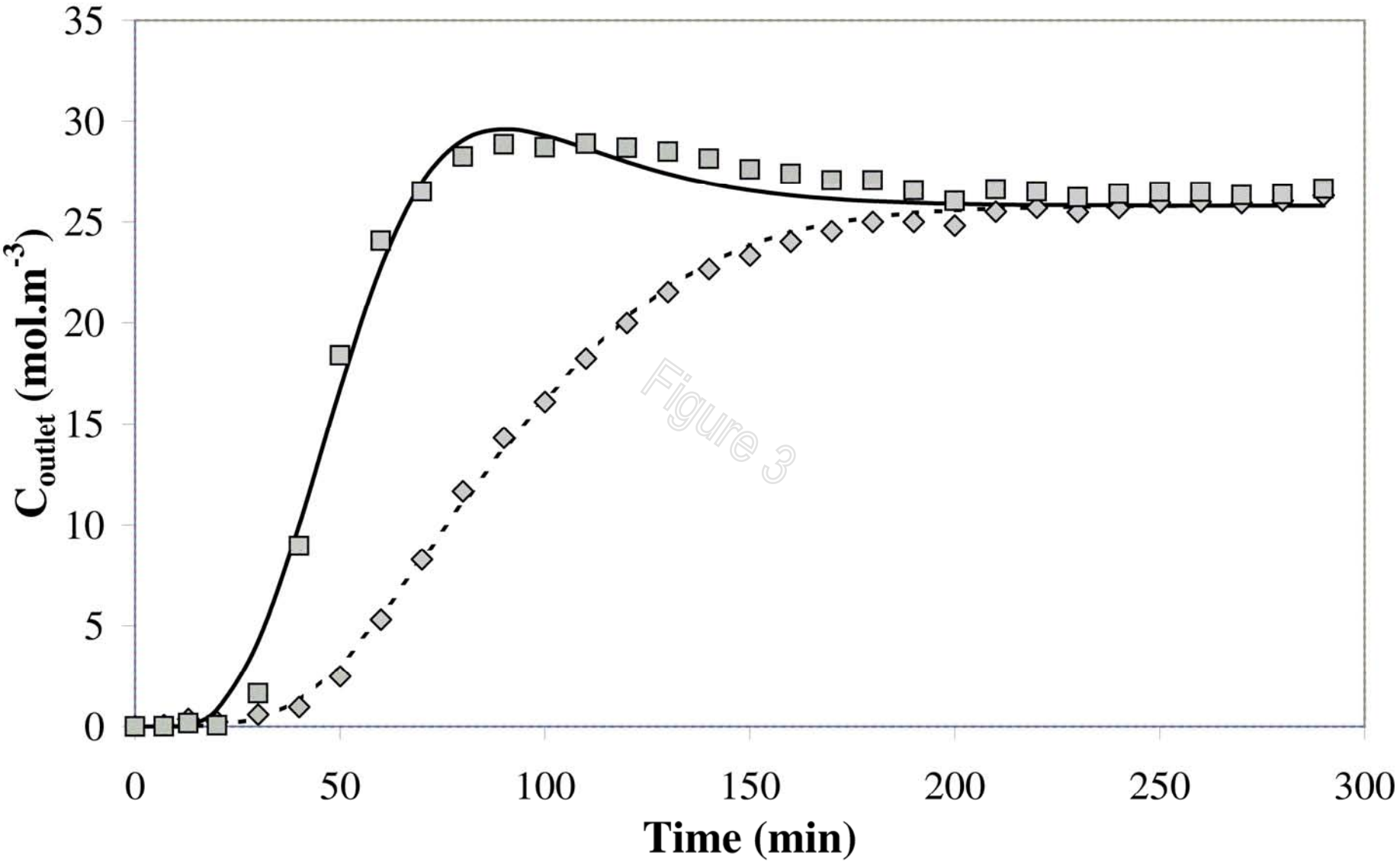
35
30
25
20
15
10
5
0
C_{outlet} (mol.m^{-3})
0
50
100
150
200
250
300
Time (min)
Figure 3

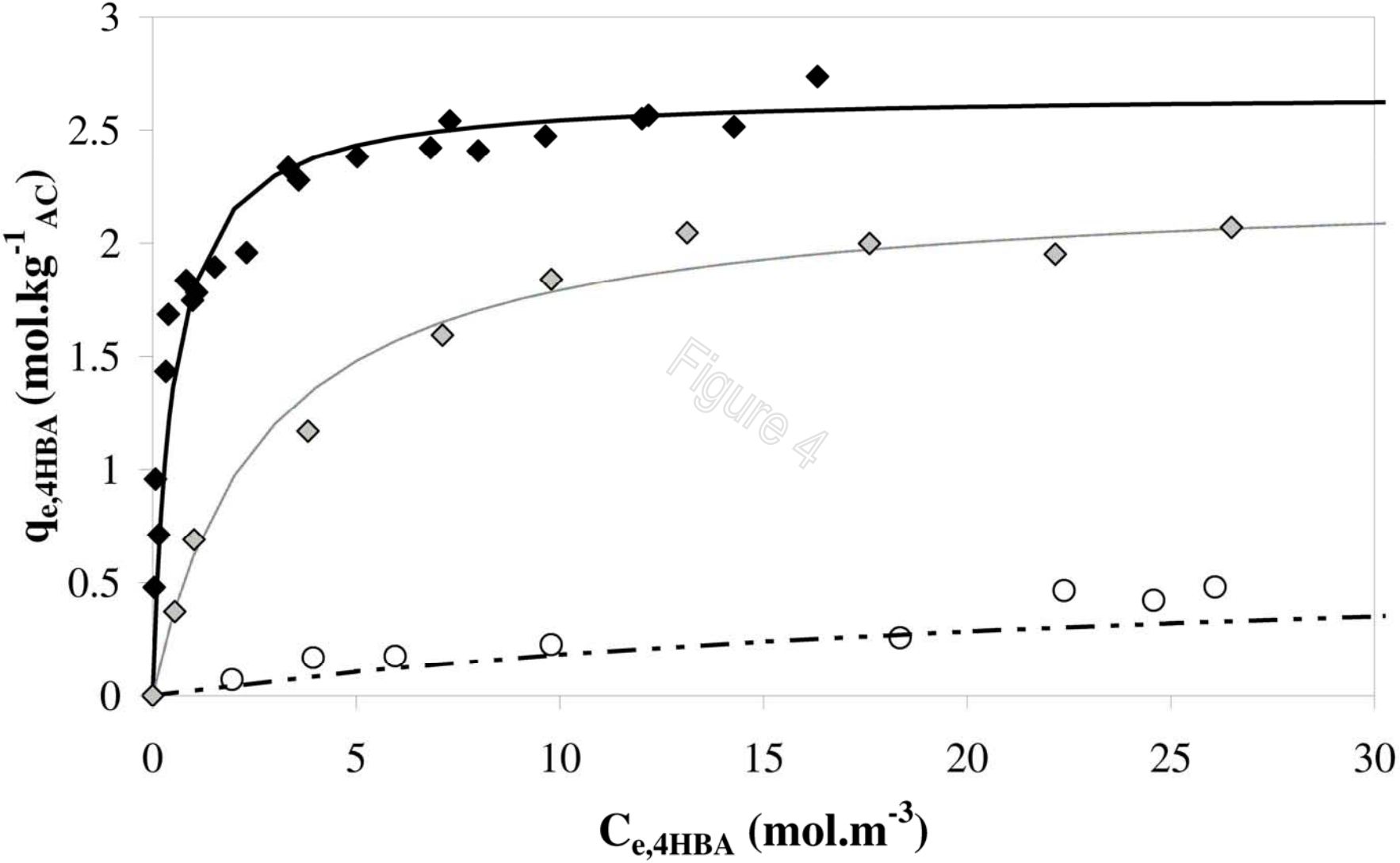
3
2.5
2
1.5
1
0.5
0
0
5
10
15
20
25
30
$q_{e,4HBA}$ (mol.kg$^{-1}_{AC}$)
$C_{e,4HBA}$ (mol.m^{-3})
Figure 4

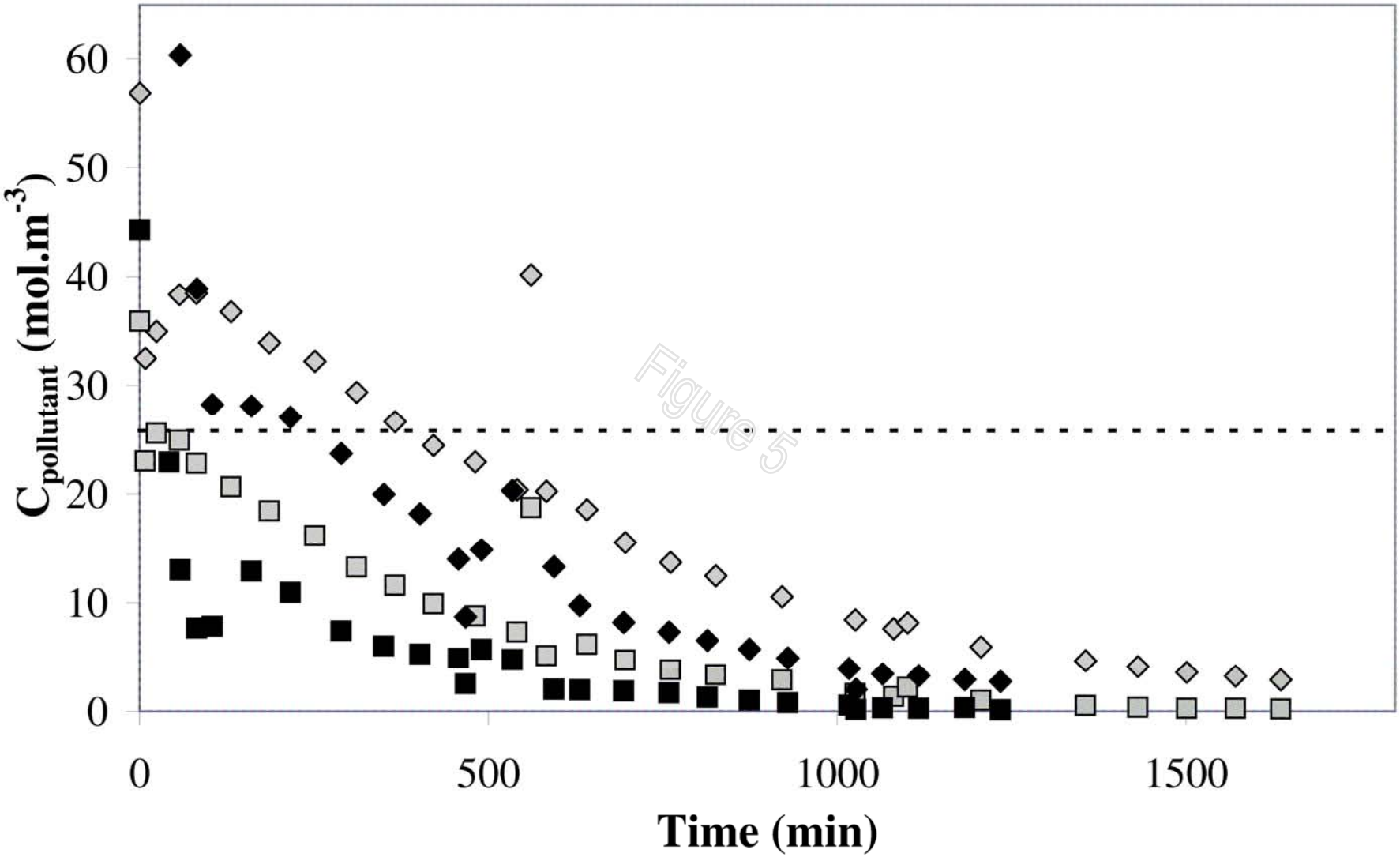

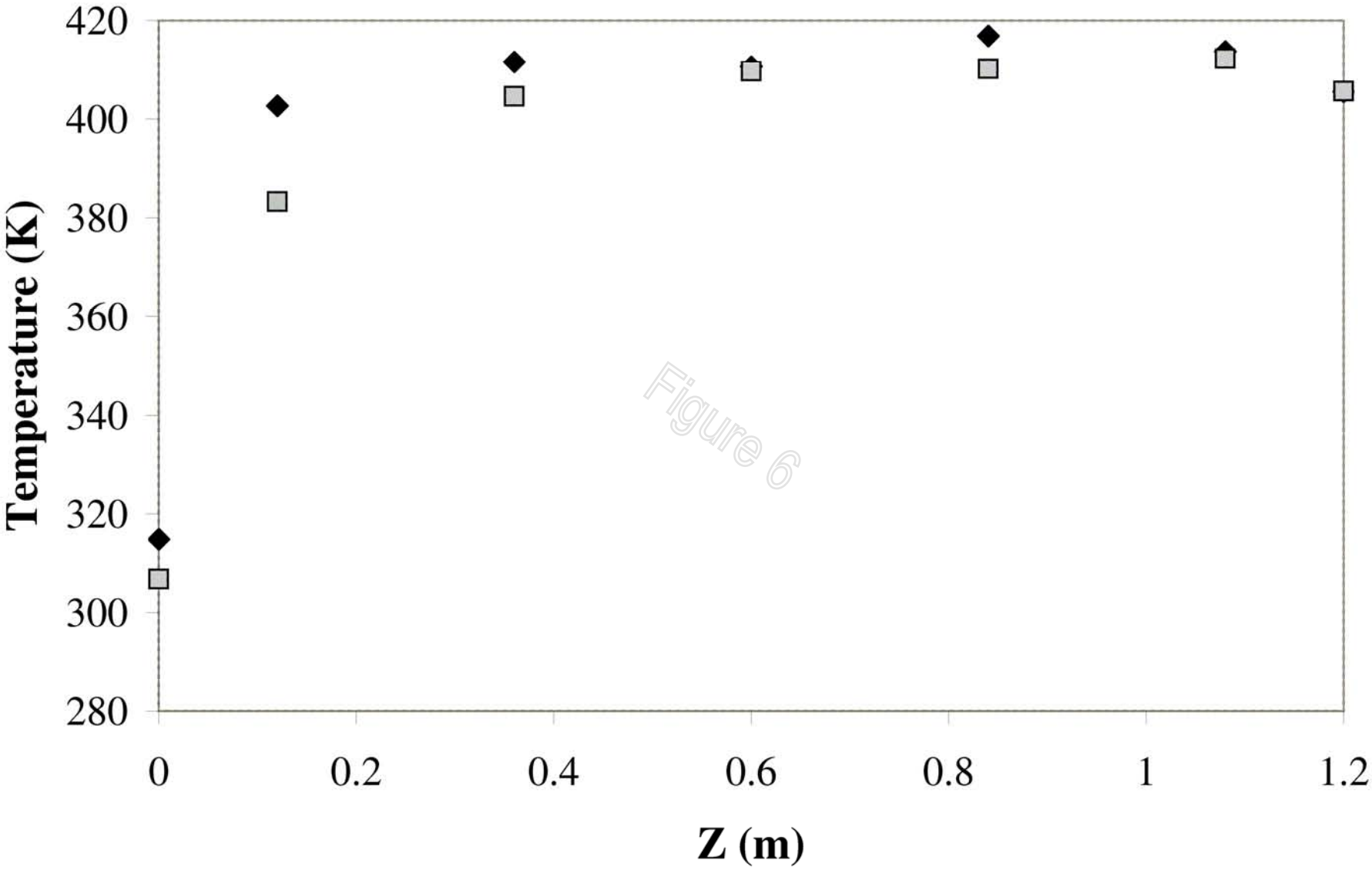
420
400
380
360
340
320
300
280
Temperature (K)
0
0.2
0.4
0.6
0.8
1
1.2
Z (m)

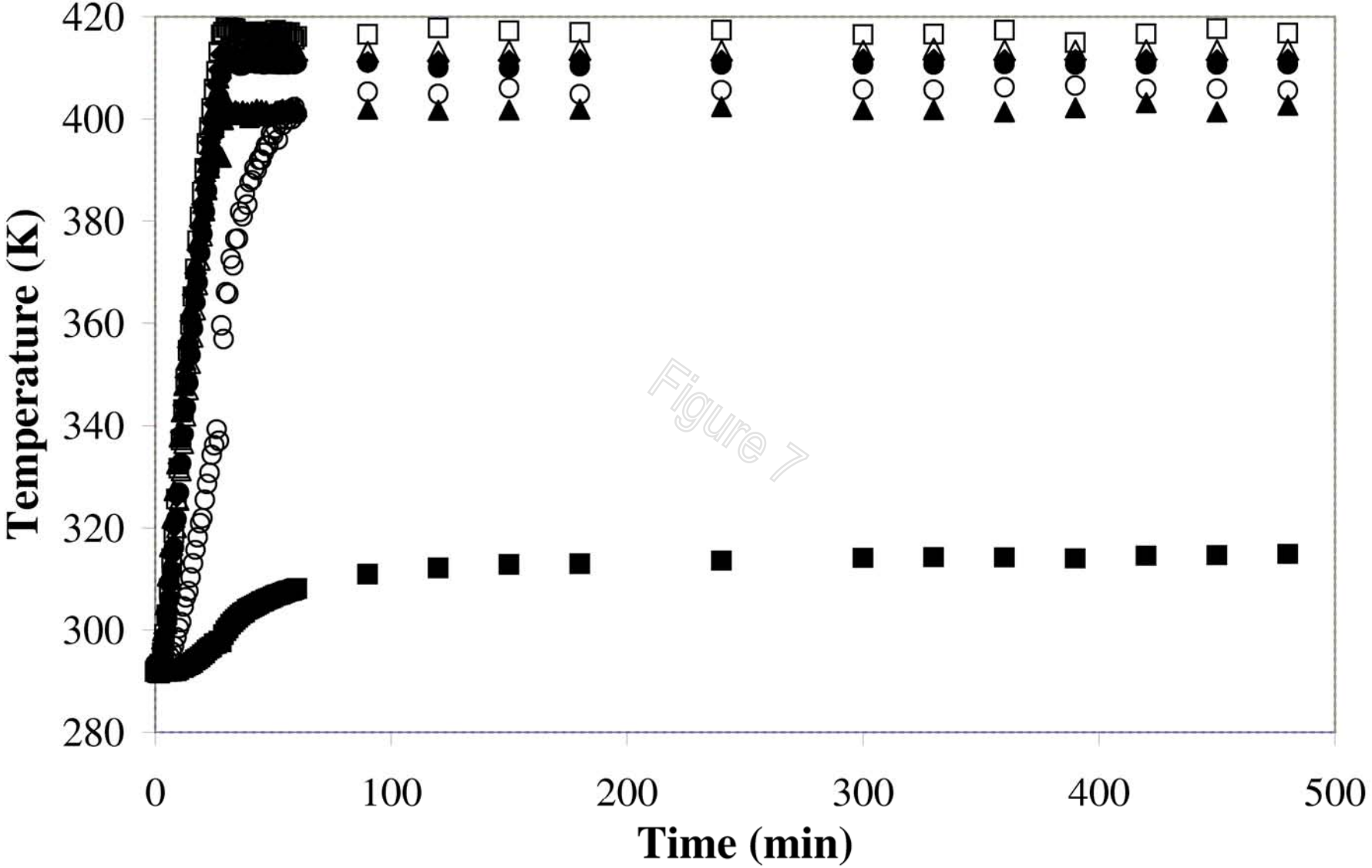
420
400
380
360
340
320
300
280
Temperature (K)
0
100
200
300
400
500
Time (min)